We are IntechOpen, the world's leading publisher of Open Access books Built by scientists, for scientists

6,900
Open access books available

185,000
International authors and editors

200M
Downloads

Our authors are among the

154
Countries delivered to

TOP 1%
most cited scientists

12.2%
Contributors from top 500 universities



WEB OF SCIENCE™

Selection of our books indexed in the Book Citation Index in Web of Science™ Core Collection (BKCI)

Interested in publishing with us?
Contact book.department@intechopen.com

Numbers displayed above are based on latest data collected.
For more information visit www.intechopen.com



5

Corrosion Resistance of Pb-Free and Novel Nano-Composite Solders in Electronic Packaging

L.C. Tsao
Department of Materials Engineering,
National Pingtung University of Science & Technology, Neipu, Pingtung,
Taiwan

1. Introduction

Tin-lead (Sn-Pb) alloys for metal interconnections were first used about 2000 years ago. Recently, the use of alloys has become essential for the interconnection and packaging of virtually all electronic products and circuits. Sn-Pb solder alloys have been widely used in the modern electronics industry because of their low melting points, good wettability, good corrosion resistance, low cost, reasonable electrical conductivity, and satisfactory mechanical properties. However, due to health concerns, recent legislation, and market pressures [1], the electronic industry is moving toward green manufacturing as a global trend. In the area of packaging, mainly driven by European RoHS (Reduction of Hazardous Substances), lead was banned effective July 1, 2006, except in some exempt items. In addition, Pb and Pb-containing compounds, as cited by the Environmental Protection Agency (EPA) of the US, are listed among the top 17 chemicals posing the greatest threat to human life and the environment [2] because of lead's toxicity [3]. In the electronics industry, the lead generated by the disposal of electronic assemblies is considered hazardous to the environment. Therefore, developing viable alternative Pb-free solders for electronic assemblies is of principal importance.

2. Lead-free solder systems

Although several commercial and experimental Pb-free solder alloys are available as replacements for Sn-Pb solders, the following families of solders are of particular interest and are the prevailing choices of industry [4]: eutectic Sn-Ag, eutectic Sn-Cu, eutectic Sn-Zn, eutectic Bi-Sn, and Sn–In, as shown in Table 1. Since the properties of the binary Pb-free solders cannot fully meet the requirements for applications in electronic packaging, additional alloying elements are added to improve the performance of these alloys. Thus, ternary and even quaternary Pb-free solders have been developed [5-7], such as Sn-Ag-Cu, Sn-Ag-Bi, and Sn-Zn-Bi solder. However, the knowledge base on Sn-Pb solders gained by experience is not directly applicable to lead-free solders. In other words, the reliability of Pb-free solder joints in consumer products is attracting more interest and concern from both academia and technologists[8-10].

All system	Eutectic composition (wt.%)	Melting point or range (˚C)
Sn-In	Sn52In	118(e)
Sn-Bi	Sn58Bi	138(e)
Sn-Zn	Sn9Zn	198.5(e)
Sn-Ag	Sn3.5Ag	221(e)
Sn-Cu	Sn0.7Cu	227(e)
Sn-Ag-Bi	Sn3.5Ag3Bi	206-213
Sn-Ag-Cu	Sn3.8Ag0.7Cu	217(e)
	Sn3.50.5Cu	218
Sn-Zn-Bi	Sn8Zn3Bi	189-199

Table 1. Data showing the enhancement of the mechanical properties of Pb-free solders[9, 10].

3. Nano-composite solders

As electronic devices continue to become lighter and thinner, they require much smaller solder joints and fine-pitch interconnections for microelectronic packaging. For example, portable electronic devices, such as portable computers and mobile phones, have become thinner and smaller while adding more complicated functions. The miniaturization of these electronic devices demands better solder-joint reliability. Hence, in all chip connection and ball grid array (BGA) technologies, solder interconnection through flip-chip assembly has been proven to offer the highest density of input/output (I/O) connections in a limited space. To meet the insatiable appetite for ever-finer I/O pitches and ever-higher I/O densities, C4 (controlled collapse chip connection) technology was developed by IBM in the mid 1960s, and this technology was applied to future microelectronic packaging. According to the International Technology Roadmap for Semiconductors (ITRS), the pad pitch may fall below 20 μm by the year 2016 [11]. In some flip chip packages, solder balls of 20μm in size are used to connect the pads on the chip and the print circuit board (Fig. 1). Furthermore, Thru-Silicon-Via (TSV) technologies are also lurking on the horizon as the next-generation higher-density chip connection technology, and they also require fine-pitch Pb-free solder interconnections.

The conventional solder technology may not guarantee the required performance at such pitches due to characteristics such as higher diffusivity and softening [12]. In order to solve these problems, efforts have been made to develop new Pb-free solders with a low melting point, good mechanical properties, better microstructure properties, and high creep resistance. Recently, Pb-free solders doped with nano-sized, nonreacting, noncoarsening oxide dispersoids have been identified as potential materials that could provide higher microstructure stability and better mechanical properties than the conventional solders [13-24]. Tsao et al. [14-16] studied the influence of reinforcing TiO_2 and Al_2O_3 nanoparticles on microstructural development and hardness of eutectic Sn-Ag-Cu solders. In their work, microhardness measurements revealed that the addition of TiO_2 and Al_2O_3 nanoparticles is helpful in enhancing the overall strength of the eutectic solder. Shen et al. [17] controlled the formation of bulk Ag_3Sn plate in Sn-Ag-Cu solder by adding ZrO_2 nanoparticles to reduce the amount of undercooling during solidification and thereby suppress the growth of bulk Ag_3Sn plates. Zhong and Gupta [18] successfully prepared a nano-Al_2O_3 reinforced nano-

composite solder by mechanically intermixing nano-Al_2O_3 particles into Sn0.7Cu Pb-free solder, and this composite solder shows improved mechanical properties. The best tensile strength realized for the composite, which contains 1.5 wt.% alumina, far exceeds the strength of the eutectic Sn–Pb solder. Many authors have studied the effect of adding single-walled carbon nanotubes [19] or multi-walled carbon nanotubes [20, 21] on the mechanical properties of nano-composite solders. The data on the enhancement of the mechanical properties of nano-composite solders collected from some of the literature are listed in Table 2 [13, 14, 16, 22, 23]. Here, it should be stressed that although the addition of nanoparticles into solder matrices can improve the creep behavior[24], the effects on the corrosion resistance and mechanical properties of the nano-composite solders cannot be ignored.

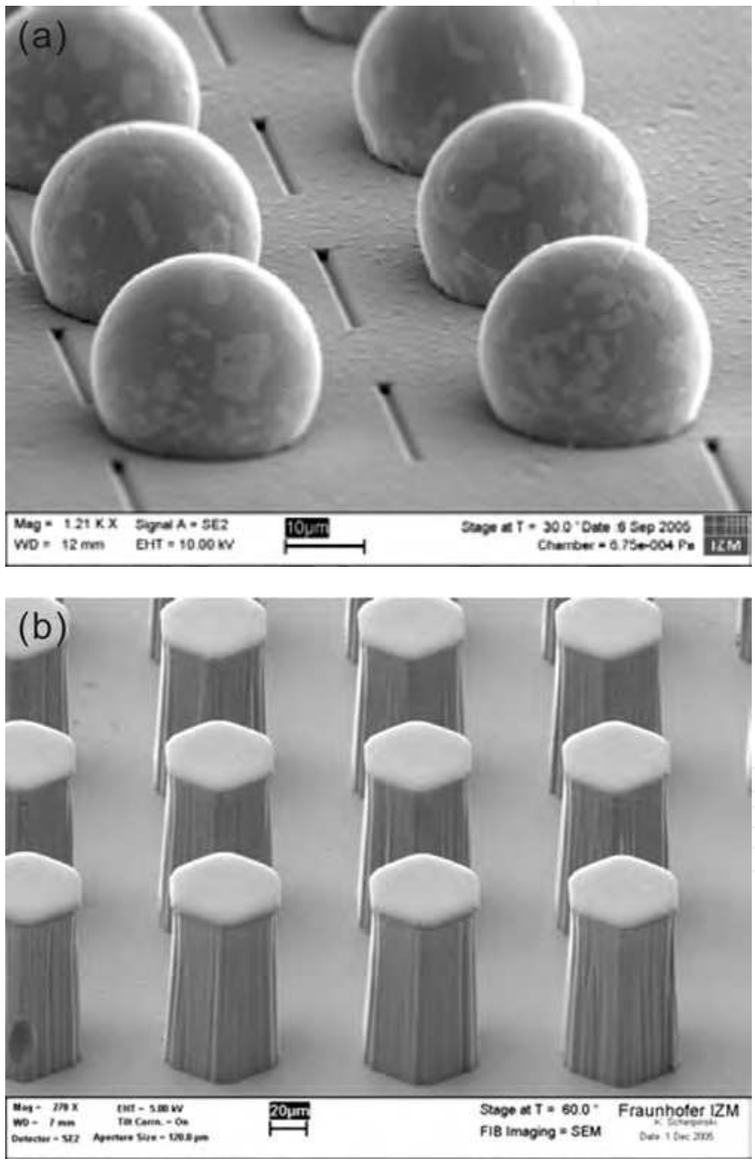


Fig. 1. Micro bump and pillar bump structures for highly reliable chip-to-substrate interconnects: (a) SnAg microbump (20 µm diameter), and (b) Cu pillarbump (height: 80 µm) [11]

Solder matrix	Reinforcement nanoparticles	Mechanical properties			
		0.2%YS (MPa)	UTS (MPa)	Elongation (%)	References
Sn4In4.1Ag0.5Cu	Nil	56±6	60±8	37±7	[22]
	1.0 vol.% Al_2O_3	72±6	75±6	21±3	
	3.0 vol.% Al_2O_3	73±3	77±6	11±3	
	5.0 vol.% Al_2O_3	74±3	76±2	10±0	
Sn3.5Ag0.7Cu	Nil	31±2	35±1	41±8	[23]
	0.01wt.% MWCNTs	36±2	47±1	36±2	
	0.04wt.% MWCNTs	36±4	46±6	37±2	
	0.07wt.% MWCNTs	33±3	43±5	35±4	
Sn3.5Ag0.5Cu	Nil	45.96±1.14	54.34±1.42	49.2±1.3	[16]
	0.25 wt.% Al_2O_3	48.81±1.23	60.20±1.84	47.3±0.8	
	0.5 wt.% Al_2O_3	52.56±1.56	62.44±1.76	44.0±1.2	
	1.0 wt.% Al_2O_3	57.22±1.8	68.05±1.63	43.5±2.1	
	1.5 wt.% Al_2O_3	61.45±2.3	70.05±2.06	32.5±3.2	
Sn3.5Ag0.25Cu	Nil	53.2	55.7	48.6	[14]
	0.25 wt.% TiO_2	59.5	61.5	40.5	
	0.5 wt.% TiO_2	67.6	69.1	32.1	
	1.0 wt.% TiO_2	69.3	70.1	25.2	

Table 2. The data showing the enhancement of the mechanical properties of nano-composite solders[13, 14, 16, 22, 23].

4. The interfacial intermetallic compound (IMC) layers

In connected metals, all the common base materials, coatings, and metallizations, such as Cu, Ni, Ag, and Au, form intermetallic compounds (IMC) with Sn, which is the major element in Sn solders. Cu is the material most frequently used for leads and pads on flip chip substrates and printed wiring boards. It is now known that in the solder/Cu interfacial reaction, Sn reacts rapidly with Cu to form Cu_3Sn (ε-phase) and Cu_6Sn_5 (η-phase) [25]. Other metal substrate/solder interfacial reactions form IMCs, such as Ag_3Sn[26] (Sn solder/Ag), Sn-Ni [27] (Sn solder/Ni), Ag-In[28] (In solder/Ag) and Cu-In IMC[29] (In solder/Cu). These intermetallic compounds are generally more brittle than the base metal, which can have an adverse impact on the solder joint reliability. Excessive thickness may also decrease solder joint ductility and strength [30-34]. Recently, we found that a great number of nano-Ag_3Sn particles form on the Cu_6Sn_5 IMC when the solders contain Ag_3Sn precipitate phase after a Pb-free Sn3.5Ag0.5Cu (SAC) nano-composite solder/Cu substrate interface reaction[30, 31]. These nanoparticles apparently decrease the surface energy and hinder the growth of the Cu_6Sn_5 IMC layer during soldering and aging. All these results indicate that Gibbs absorption theory can be used to explain the formation of these nanoparticles and their effects on the surface energy of the IMC. Many studies have reported that nano-sized, nonreacting, noncoarsening oxide dispersoid particles, such as TiO_2 [30-32], Al_2O_3 [33], Y_2O_3[34], CNTs [35], and ZrO_2[36] can affect the growth rate of interfacial IMC.

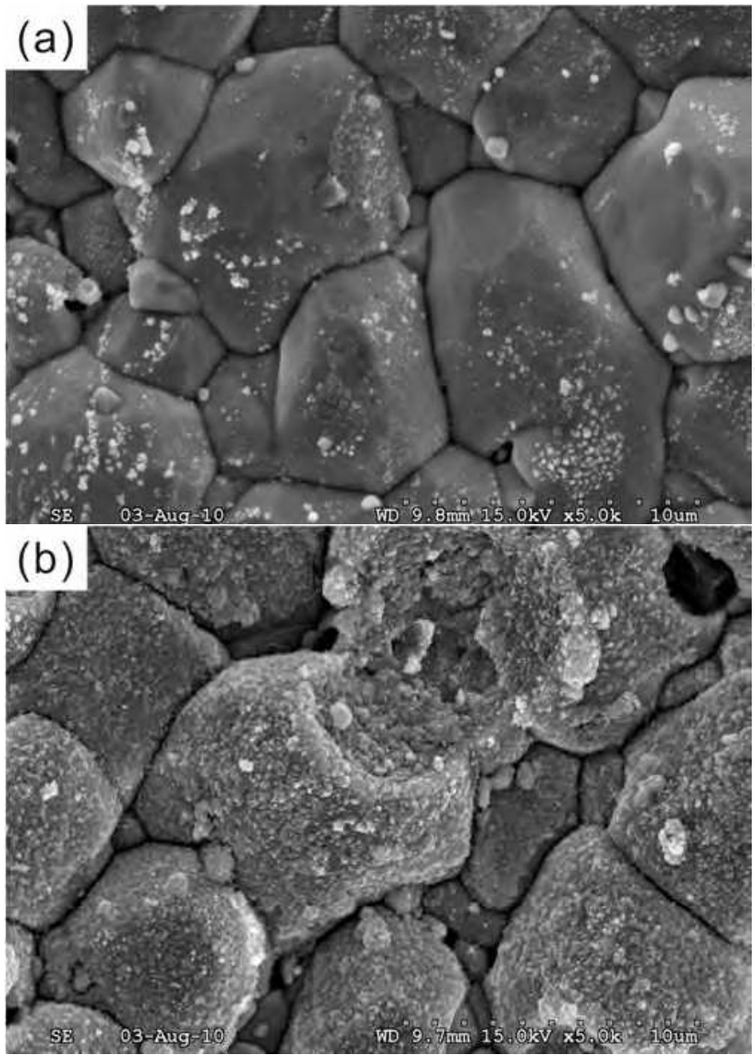


Fig. 2. Top view of the IMC at the interfaces of the nano-composite solder joints on Cu substrate after aging for 7 days at 175°C: (a) SAC and SAC- TiO_2 [31].

5. Corrosion behavior of Pb-free solder joints

The diversity of materials, drive toward miniaturization, and globalization have significantly contributed to the corrosion of microelectronic devices [37]. However, the key point is that solder joints are often exposed to corrosive environments that can accelerate the corrosion process. Although corrosion resistance is an important parameter in choosing solder alloys, the corrosion behavior of Sn-Pb solder joints was rarely of interest because the oxide that forms on the tin-lead alloy is relatively stable. Mori et al. showed that both Pb-rich and Sn-rich phases dissolve when the Sn-Pb solder alloy is immersed in corrosive solution, and the corrosion rate is slower than that of the Sn-Ag solder [38, 39]. Compared to traditional Sn-Pb solders, Sn-Ag-Cu solders are easily corroded in corrosive environments due to their special structures (as shown in Fig. 3). The presence of Ag_3Sn in Sn-Ag-Cu solders accelerates the dissolution of tin from the solder matrix into a corrosive medium

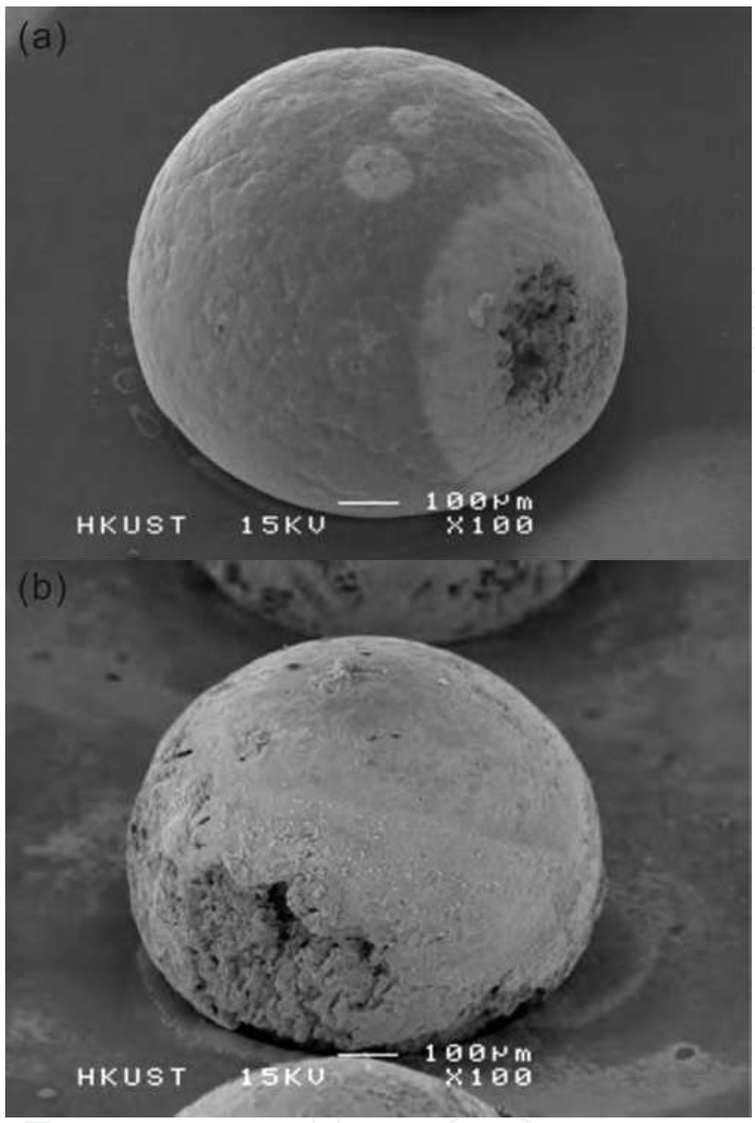


Fig. 3. Surface morphology changes of solder balls after the salt spray test for 96 hrs: (a) Sn-Pb solder, and (b) SAC solder[39].

because of the galvanic corrosion mechanism [39]. When corrosion occurs in the solder joints, it may change the microstructure of corroded regions and provide crack initiation sites, thereby decreasing the mechanical properties of the joints. Lin and Lee have investigated both Sn-Pb and Sn-Ag-Cu solder alloy wafer-level packages, with and without pretreatment by 5% NaCl salt spray, with thermal cycling to failure. The salt spray test did not reduce the characteristic lifetime of the Sn-Pb solder joints, but it did reduce the lifetime of the Sn-Ag-Cu solder joints by over 43% (Fig.4). The characteristic lifetime cycle number was 1384 for the as-assembled and non-salt spray treated components, but it was only 786 for the components which were treated in 5 wt.% NaCl salt spray for 96 h. In addition, the presence of multiple corrosion sites per solder joint poses an additional risk factor to the structural stability of the joint, for corrosion sites are all potential crack initiation sites.

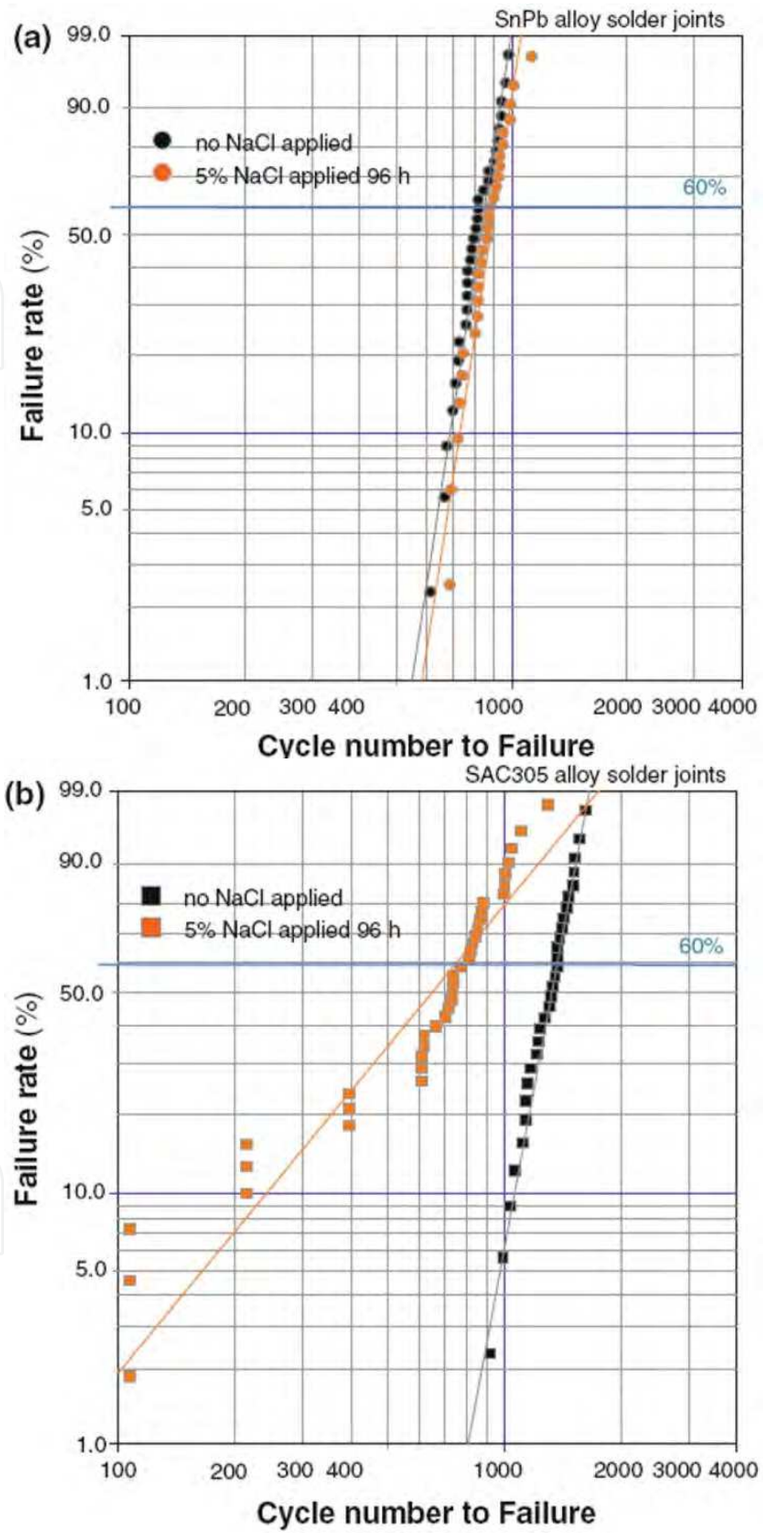


Fig. 4. Weibull plot for the thermal cycling results on 5 wt.% NaCl aqueous solution (salt spray) treated WLCSP: (a) Sn-Pb solder alloy samples and (b) SAC305 solder alloy samples [40].

Unlike Sn-Pb joints, which have a dual phase structure and block the path of corrosion due to the existence of phase boundaries, the SAC305 joint is basically pure Sn with coarse islands of Ag_3Sn and Cu_6Sn_5 intermetallic precipitate (Fig. 5). A corrosion crack can propagate and lead to additional corrosion along the way, without interruption from the Sn phase structure. Although both materials show strong resistance to corrosion, the localized nature of the corroded area at critical locations causes significant degradation in Sn-Ag-Cu solder joints[40].

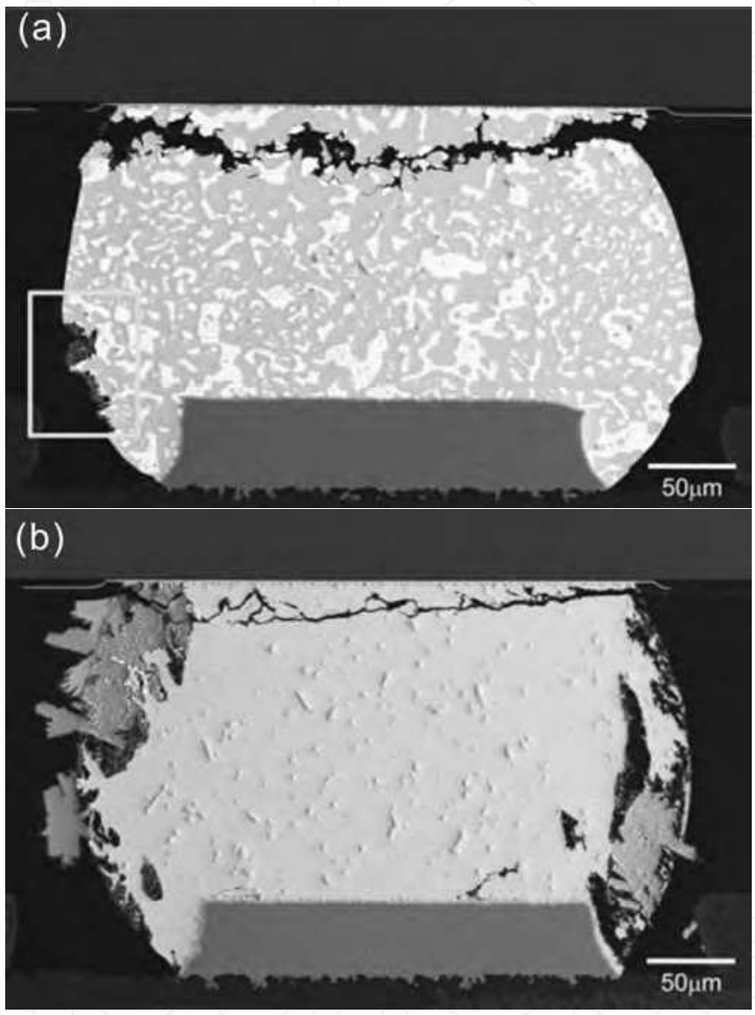


Fig. 5. Cross-section SEM microstructure after salt spray treatment and then thermal cycling: (a) Sn-Pb, and (b) SAC305 solder joint [40].

6. Galvanic corrosion of soldering

Corrosion of solder alloys, in the presence of a suitable electrolyte can occur either due to the potential difference between the major phases in the alloy or galvanic coupling between one or more phases of the alloy and other parts of the microelectronics device. Some metals that are frequently used in microelectronics are Cu, Au, Ag, Ni and Pd. The standard emf for these metals and metals used in solder alloys are listed in Table 3[4]. Especially, advanced packaging technologies make the solder alloy susceptible to corrosion problems

[41]. Thus, in the electronics industry, corrosion has become a significant factor in recent years because of the extremely complex systems that have been developed and the increasing demand on their reliability [42, 43]. For example, using Cu and Sn metals allows fine-pitch interconnections to be fabricated at relatively low cost. These features make Cu-Sn based SLID bonding very appealing for 3D stacked applications (Fig. 6) [44].

Metals used in solder	**Metals used in microelectronics**				
	Au	Ag	Cu	Ni	Pd
Sn	1.636	0.935	0.473	-0.114	1.123
Pb	1.626	0.925	0.463	-0.124	1.113
In	1.842	1.141	0.679	0.092	1.329
Zn	2.263	1.562	1.10	0.513	1.75

Table 3. Δemf values for metals commonly used in microelectronics[4].

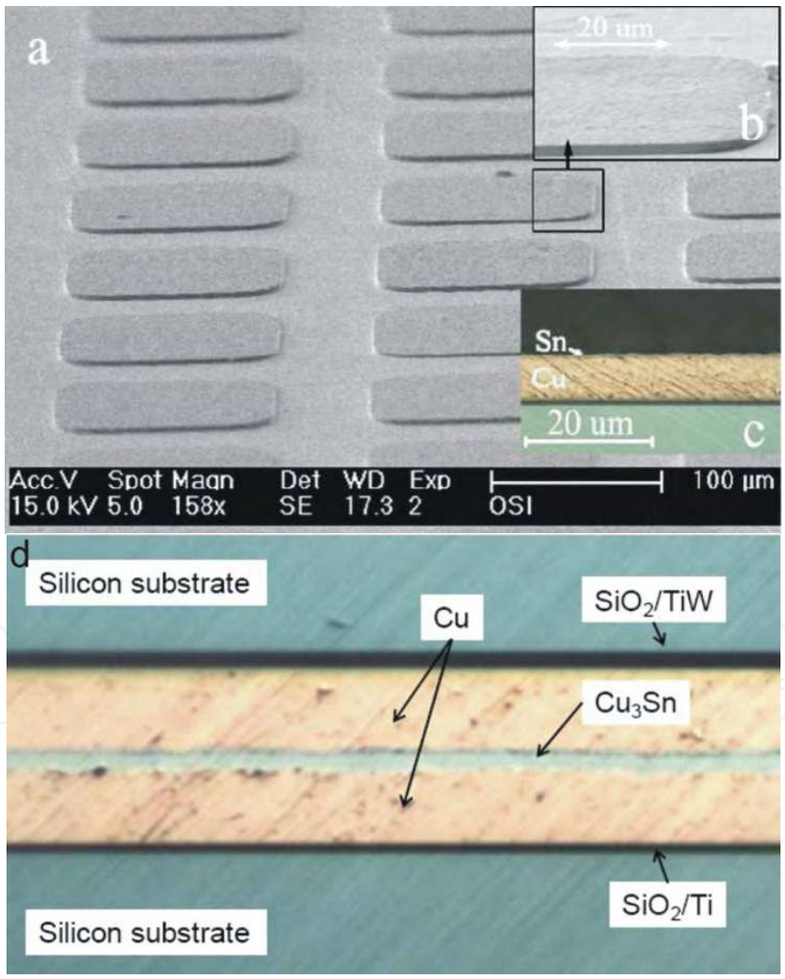


Fig. 6. Electroplated pads of 5 µm Cu and 200 nm Sn: (a) and (b) SEM image with different magnification; (c) Cross-section view under optical microscope; and (d) Cross-section view of a fluxless bonded Cu/Sn Interconnect [44].

The joining of materials with solders generally results in a multi-layer structure in which IMC are formed between substrate and solders. Such a structure in a flip chip package is a galvanic couple. The galvanic corrosion behavior of the solder bump structures have a great effect upon reliability[45]. For instance, the galvanic current densities of the Sn solder with respect to the IMC Cu_6Sn_5 and Cu_3Sn, and base Cu have been investigated (Fig. 7). It appears that Sn solder has a greater galvanic current density and thus is very subject to corrosion, and it is especially so in coupling with the formation of Cu_3Sn layers than with Cu_6Sn_5 layers. The galvanic current densities of the Sn37Pb solders of Cu_3Sn, Cu, and Cu_6Sn_5 are about 38, 16, and 5 ($\mu A/cm^2$), respectively.

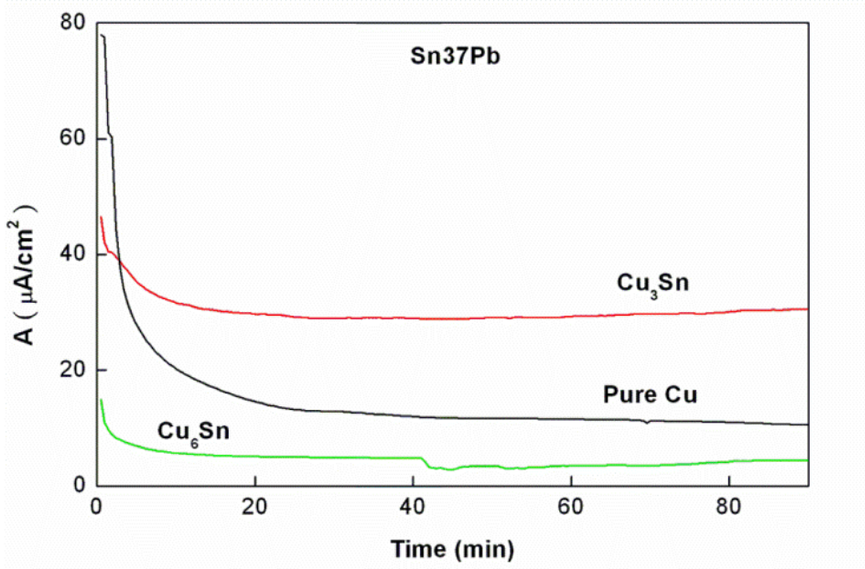


Fig. 7. The galvanic current densities of the solder with respect to intermetallic compounds Cu_6Sn_5 and Cu_3Sn, and Cu substrate, in a 3.5 wt.% solution [45].

Increasing the copper content, which reacts with Sn to form IMC, significantly improves the corrosion resistance of solders and increases the corrosion current density (I_{corr}), as shown in Fig. 8, 9 and Table 4. At above 460 mV_{SCE}, the passivation current densities of all specimens are around $10^{-1} A/cm^2$, with the declining sequence of Sn37Pb ≥ Cu_6Sn_5 > Cu_3Sn > Cu.

Specimens	Φ_{corr} (mV_{SCE})	Φ_b (mV_{SCE})	$\Delta\Phi$ (mV)	I_{corr} ($\mu A/cm^2$)	I_p (mA/cm^2)
Sn37Pb	-584.4	-303.0	281	6.48	67.7
Cu_6Sn_5	-457.7	-45.0	412	2.61	56.9
Cu_3Sn	-309.0	-8.9	300	48.17	18.3
Cu	-192.1	236	428	391.6	6.5

$\Phi_{corr.}$: corrosion potential; $I_{corr.}$: corrosion current density; Φ_b : breakdown potential;
$\Delta\Phi = \Phi_{corr.} - \Phi_b$, Φ_p: passivation range of solder alloy;
I_p: passivation current density at above 460 mV_{SCE}.

Table 4. Corrosion properties in a 3.5 wt.% NaCl solution for the Sn37Pb solder, Cu_6Sn_5 IMC, Cu_3Sn IMC and pure Cu samples [45].

It can be seen that the galvanic corrosion behavior of Cu_3Sn is generally greater than that of Cu_6Sn_5 for the flip chip package in a 3.5 wt. % NaCl solution environment. This indicates that the formation of IMC Cu_3Sn and Cu_6Sn_5 layers causes many problems with corrosion behavior and reliability.

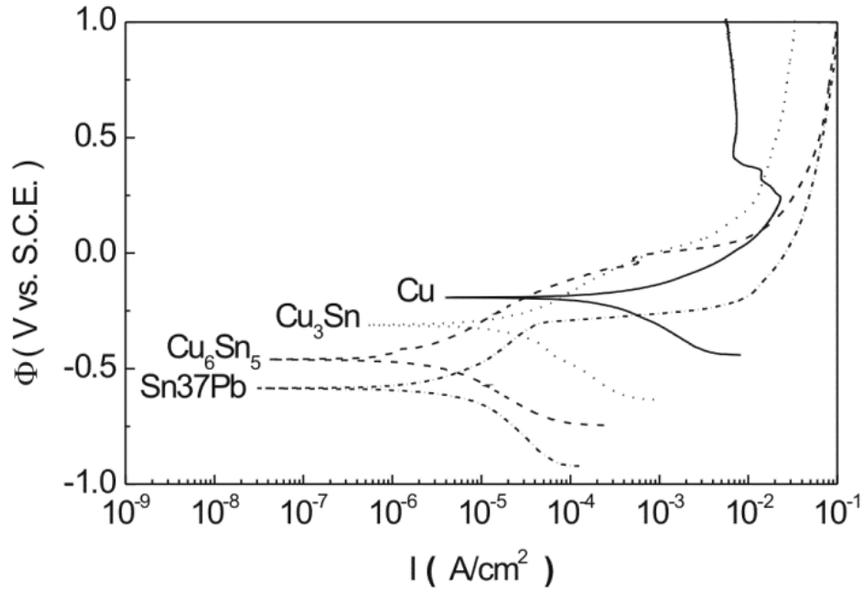


Fig. 8. The potentiodynamic polarization curves of Sn37Pb solder, Cu_6Sn_5 IMC, Cu_3Sn IMC, and pure Cu samples in a 3.5 wt.% NaCl solution [45].

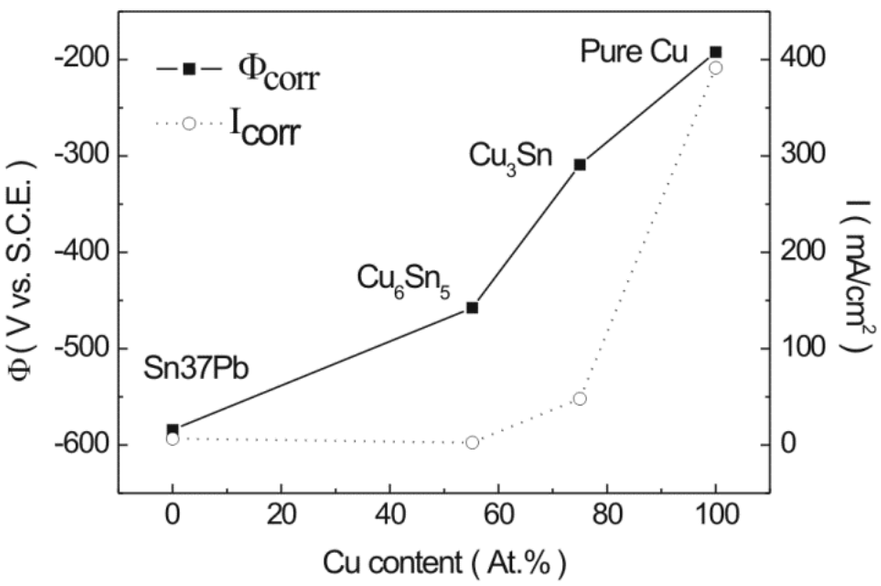


Fig. 9. Effect of Cu content on both Φ_{corr} and I_{corr} during polarization of the Sn37Pb solder, Cu6Sn5, Cu3Sn, and Cu substrate in 3.5 wt.% NaCl solution[45].

7. Corrosion behavior of Pb-free solder

Both the particular design of the electronic system, and the manner in which it is mounted in a substrate or printed wiring board, the solder connection can be exposed to the atmosphere. The solder is thus not only exposed to air, but also moisture and other corrosives such as chlorine and sulfur compounds. The ability of the solder to be able to withstand corrosion property is therefore relevant to the long-term reliability of solder joints [4]. In addition, solder alloys are electrically connected with other metallic components in the electronic device. Some metals that are frequently used in microelectronics are Cu, Au, Ag, Ni and Pd. Therefore, there is also the potential for galvanically induced corrosion of the solder, which could exacerbate any atmospheric corrosion that might be occurring. However, the properties of these lead free alloys in corrosive environments has not been widely reported, though it is of importance in many automotive, aerospace, maritime and defence applications [46]. Some researchers have studied the corrosion behaviour of Sn–Zn–X solders [47, 48] and Sn–Zn–Ag–Al–XGa [49], but few [50, 51] have studied the corrosion properties of Sn–Ag, Sn–Cu and Sn–Ag–Cu solders. Zinc is both metallurgically and chemically active. The presence of Zn in the solder alloy results in poor corrosion resistance, which is an important problem to address before practical application of this material [49]. Hence, the electrochemical corrosion behaviour of Pb-free Sn-Zn binary solder and Sn-Zn-X (X=Bi, Ag and Al) solder alloys have been investigated in NaCl solution by potentiodynamic polarization techniques[52-55]. Lin et al. [47-49] have investigated the corrosion behaviour of Sn–Zn–Al, Sn–Zn–Al–In and Sn–Zn–Ag–Al–XGa solders in 3.5% NaCl solution. They found that Sn–Zn–Al alloy [47] undergoes more active corrosion than Sn–37Pb alloy. Furthermore, they found that 5In–9(5Al–Zn)–YSn and 10In–9(5Al–Zn)–Sn alloys exhibit electrochemical passivation behaviour, and the polarization behaviours of these two alloys are similar to that of 9(5Al–Zn)–Sn alloy. Sn-Ag-M (M=In, Bi) solders exhibit poor corrosion behaviour as compared to that of Sn-Pb eutectic solder (0.1M NaCl solution)[56]. In contrast, increasing the copper content (from 0.8 to 6.7 at.%) enhances the corrosion resistance of Sn-Ag solder alloys, which exhibit improved passivity behaviour as compared to Sn-Pb eutectic solder. EPMA results indicate that the Ag_3Sn IMC is retained after the polarization test. Hence, the Ag_3Sn is more noble than the β-Sn phase. The pit formation on the surface of Sn–Ag–M alloys is due to the dissolution of the tin-rich phase. Wu et al. [51] has studied the corrosion behaviors of five solders in salt and acid solutions by means of polarization and EIS measurements. The Sn3.5Ag0.5Cu solder has the best corrosion resistivity due to the high content of noble or immune elements (Ag and Cu) and theorized stable structure, whereas the Sn9Zn and Sn8Zn3Bi solder have the worst corrosion behavior. Nevertheless, the four Pb-free solders exhibit acceptable corrosion properties, since there is not much difference in key corrosion parameters between them and the Sn37Pb solder. The corrosion data of the solders in 3.5 wt.% NaCl solutions are listed in Tables 5 [46, 51]. Lin and Mohanty et al. [46-49] studied the corrosion properties of Sn–Zn–X and Sn–Zn–Ag–Al–XGa in NaCl solution, and their results showed that the corrosion product on the surface could be SnO, SnO_2, $SnCl_2$ and ZnO, etc., depending on the applied potential. Li et al. [46] confirms that the corrosion product on the Sn–Pb and lead free solders is tin oxide chloride hydroxide ($Sn_3O(OH)_2Cl_2$).

Solder	Scanning rate	*E*corr (mV)	*I*corr (A/cm²)	E_p (mV)	I_p (mA/cm²)	References
Sn37Pb	1 mV/s	-588	1.905×10^{-6}	-201	4.989	[51]
Sn9Zn		-940	2.691×10^{-5}	-326	2.938	
Sn8Zn3Bi		-1291	1.380×10^{-5}	9	8.035	
Sn3.5Ag0.5Cu		-605	5.370×10^{-7}	-236	4.083	
Sn3.5Ag0.5Cu9In		-578	7.413×10^{-6}	-158	1.524	
Sn0.7Cu	30 mV/s	-688	1.78×10^{-7}	-	0.74	[46]
Sn3.5Ag		-705	4.9×10^{-7}	-	0.49	
Sn3.8Ag0.7Cu		-727	0.89×10^{-7}	-	1.07	

Ecorr – corrosion potential, Ip – passivation current density, Icorr – corrosion current density, Ep – passive potential.

Table 5. Experimental data of the testing solders under polarization in 3.5 wt.% NaCl solution.

8. Corrosion behavior of Pb-free nano-composite solder joints

This author has recently worked on the development of nano-composite solders in microelectronic packaging by applying two methods of fabrication: mechanical mixing of inert nano-particles (Fig. 10) and precipitation of nano-IMC in the solder matrix (Fig. 11) [57]. The average size of the nominally spherical nano-Al_2O_3 particles was 100 nm in diameter.

Notably, the addition of nano-particles decreased the size of dendrite β-Sn grains, the needle-like Ag_3Sn grains, and Ag_3Sn phase located between the average spacing. When 1 wt% was added, the superfine spherical nano-Ag_3Sn grains were about 0.16 ± 0.06μm in length and 0.15 ± 0.05 μm in diameter, and the average spacing between them was a significant improvement (0.14 ± 0.05μm), significantly smaller than the sizes found in the SAC composite solder. However, large Ag_3Sn IMCs were not observed in the Pb-free SAC solder. Another, author reported that the effects of nano-TiO_2 particles on the interfacial microstructures and bonding strength of Sn3.5Ag0.5Cu nano-composite solder joints in ball grid array (BGA) packages with immersion Sn surface finishes [58]. It is clearly shown in Fig. 12a, b that the discontinuous Cu_6Sn_5 IMC layer grows with a rough scallop shape (Mark A), and wicker-Cu_6Sn_5 IMC forms on the rough scallop-shaped Cu_6Sn_5 IMC layer (Mark B) and grows into the SAC solder matrix. However, the addition of a small percentage of nano-TiO_2 particles alters the Pb-free Sn3.5Ag0.5Cu composite solder/pad interface morphology after reflowing, as shown in the SEM micrographs in Fig. 12c, d. Only the continuous scallop-shaped Cu_6Sn_5 IMC layer was detected at the interface. However, the wicker-Cu_6Sn_5 IMC disappeared at the interface with the Cu pads. In addition, the number of Ag_3Sn IMC forms increased in the eutectic area when the content of nano- TiO_2 particles was increased to 0.25–1 wt%. It is interesting that the smallest

thickness of the IMC layer was achieved with the addition of 1 wt% of nano-TiO_2 particles. The thickness of the Cu_6Sn_5 IMC layer was reduced by 51%. The results indicate that the growth of the Cu_6Sn_5 IMC layer at the solder/pad interfaces of Sn3.5Ag0.5Cu is depressed through the small addition of nano-TiO_2 particles[58]. With the addition of 0.5–1 wt% nano-TiO_2 particles, fracture occurred in all of the solder joints as cracks propagated through the Sn3.5Ag0.5Cu composite solder balls, which ruptured mostly along the submicro Ag_3Sn IMC and solder matrix, as shown in Fig. 13a, b. This phenomenon is similar to that occurring in Pb-free Sn0.7Cu composite solder BGA packages[59].

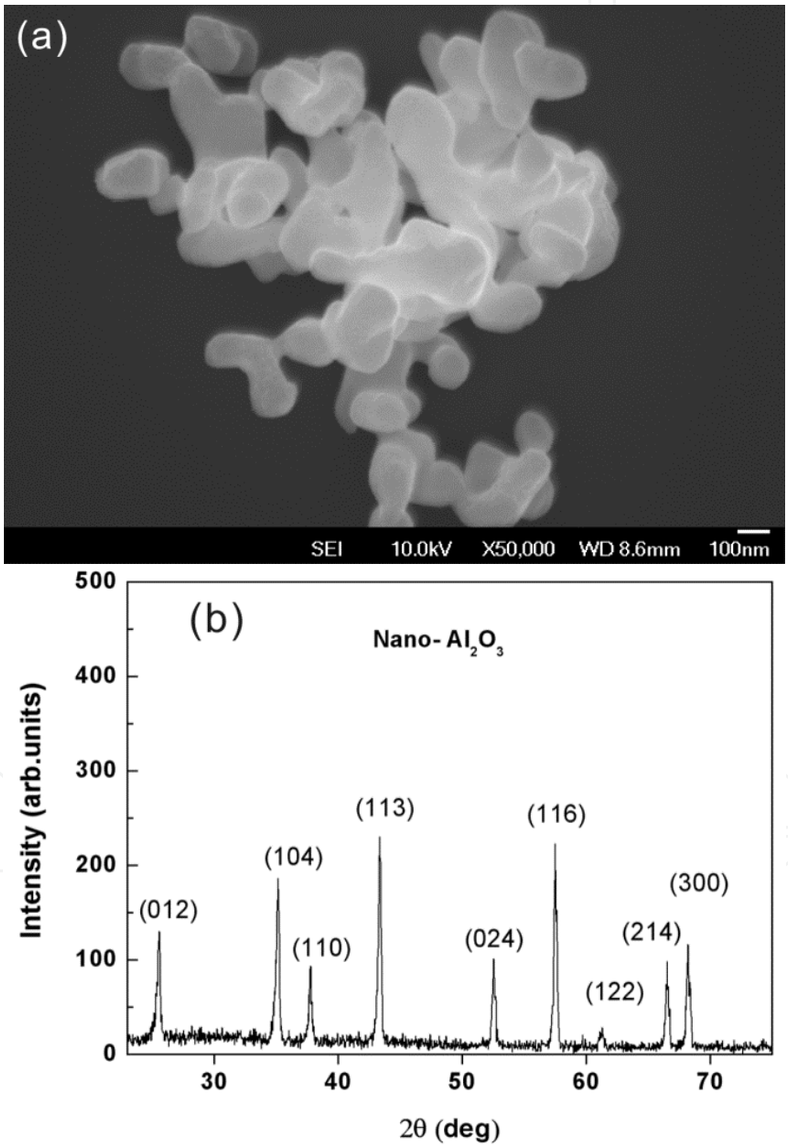


Fig. 10. The nano-Al_2O_3 particles used in this study: (a) FE-SEM micrograph, and (b) X-ray diffraction spectrum[57].

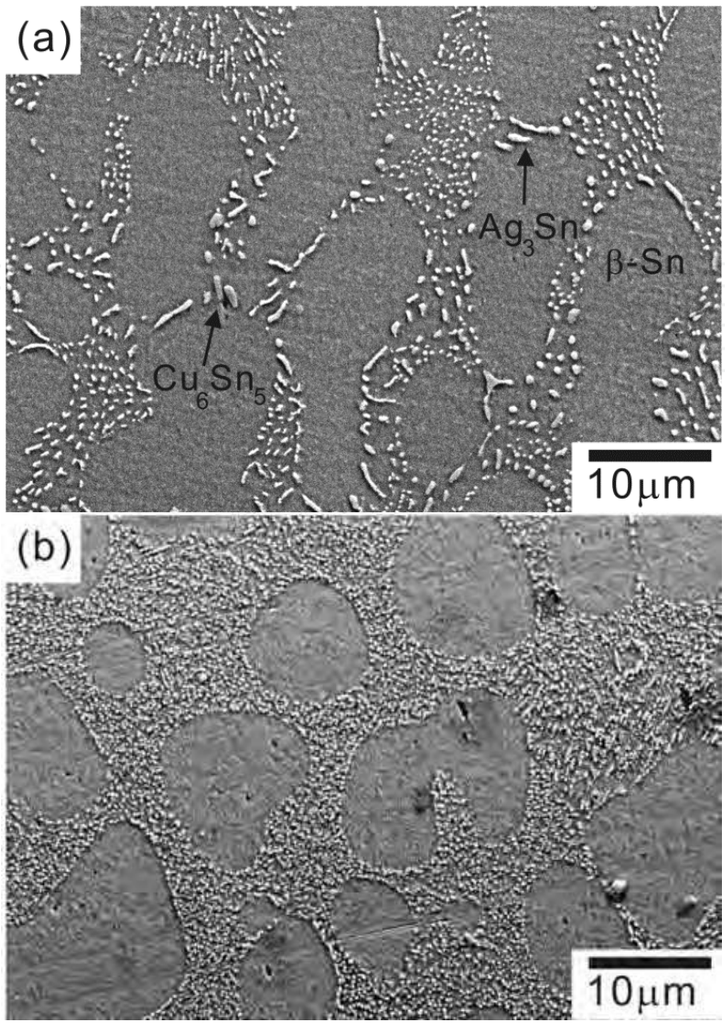
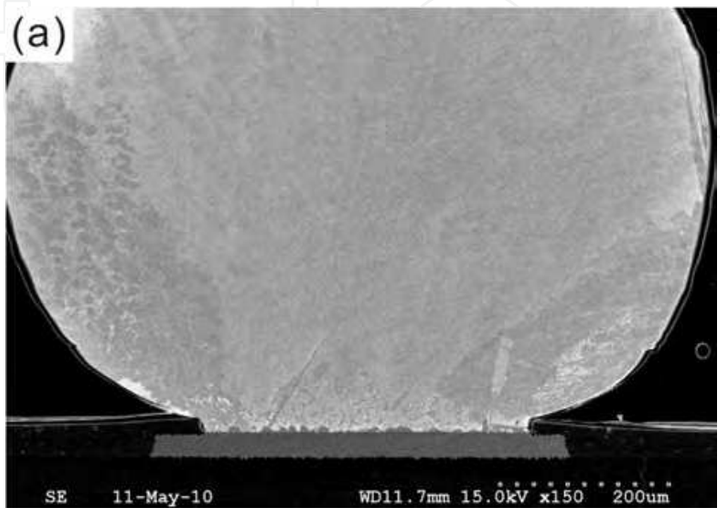


Fig. 11. SEM image of the (a) Sn3.5Ag0.5Cu solder and (b) Sn3.5Ag0.5Cu -1TiO_2 nano-composite solder[57].



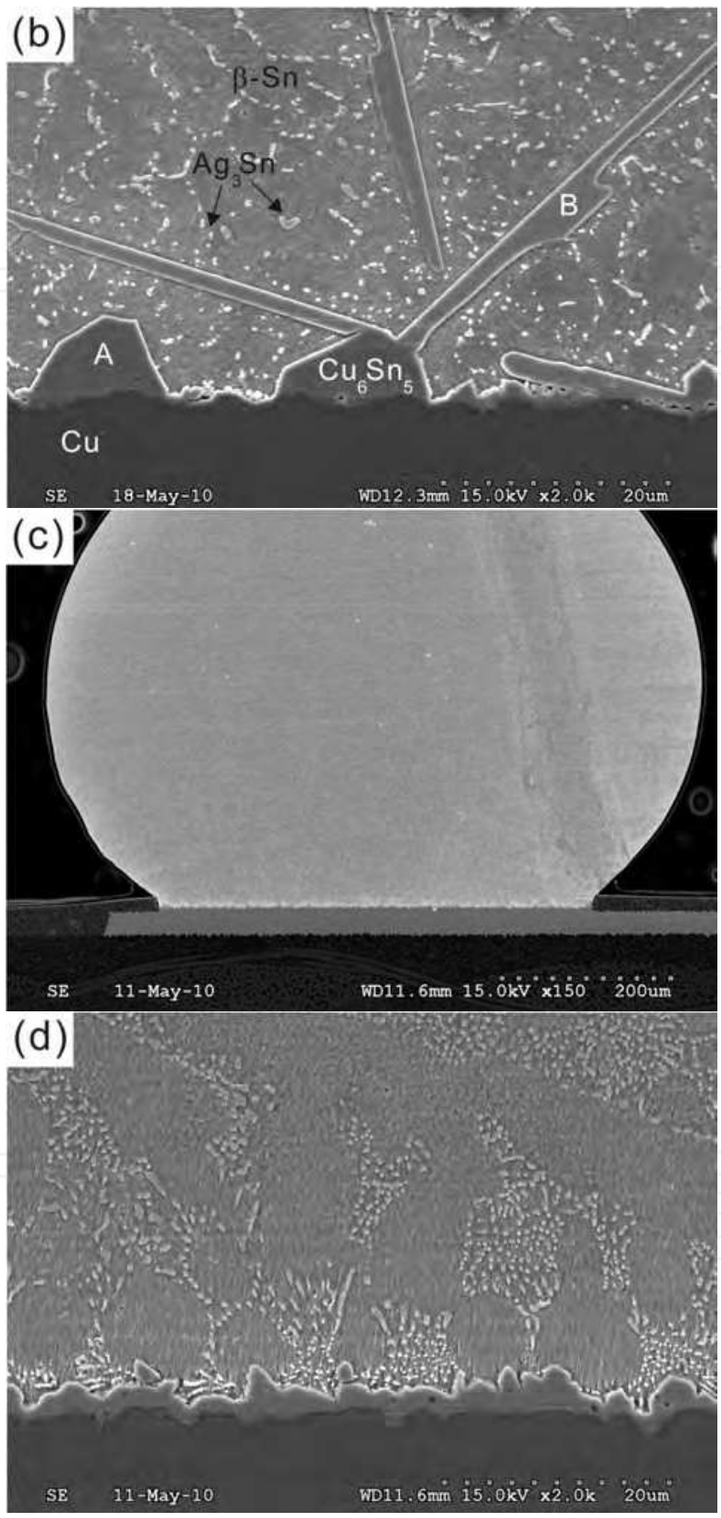


Fig. 12. Morphology of intermetallic compounds formed at the interfaces of the as-reflowed solder joints: (a) Sn3.5Ag0.5Cu, (b) (a) magnifications ; (c) d Sn3.5Ag0.5Cu-0.75TiO_2; (d) (c) magnifications [58].

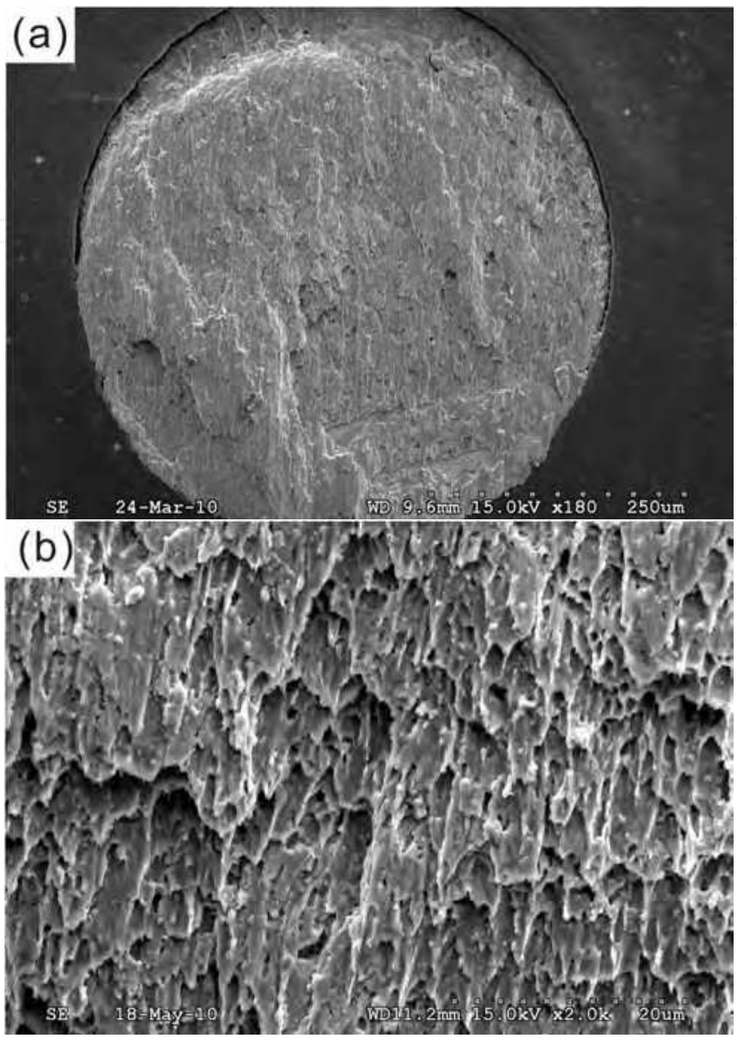


Fig. 13. Fractography of the Sn3.5Ag0.5Cu-1TiO_2 nano-composite solder joints in BGA packages after ball shear tests [58].

To achieve high reliability, solder materials must have high resistance to corrosive conditions such as moisture, air pollutants from industry, and oceanic environments[54]. Although corrosion of solder alloys is not currently a major problem for electronic devices used in normal environments, it may be a problem when they are used in harsh environments, such as oceanic environments. However, there is a lack of information regarding the corrosion resistance of nano-composite solders in corrosive environments.

Figure 14 shows the polarization curves of the Sn3.5Ag0.5Cu solder and the Sn3.5Ag0.5Cu nano-composite solder in 3.5 wt.% NaCl solution[60]. From the polarization curves, the corrosion potential (Φcorr), the breakdown potential (Φ_b), and the dynamic corrosion current density (Icorr) have been determined (Table 6). The width of the passive region on the anodic polarization curves ($\Delta\Phi = \Phi_b - \Phi$corr) in Table 6 indicates the pitting

resistibility or the stability of the passive film on the Sn3.5Ag0.5Cu composite alloy surface. The corrosion potential (Φcorr) of the Sn3.5Ag0.5Cu nano-composite solder is slightly more passive than that of the Sn3.5Ag0.5Cu solder. This implies that a finer grain size produces more grain *b*oundaries, which act as corrosion barriers. On the other hand, the breakdown potential (Φ_b) of the Sn3.5Ag0.5Cu nano-composite solders becomes much more passive with the addition of oxide nanoparticles. As Table 6 also indicates, the Sn3.5Ag0.5Cu solders possess a higher pitting tendency (smaller $\Delta\Phi$ value) than the Sn3.5Ag0.5Cu nano-composite solders. Rosalbino et al. reported that the pit formation at the surface of Sn–Ag–M alloys is due to the dissolution of the tin-rich phase [56]. In addition, the corrosion current densities were obtained by using the TAFEL extrapolation method. The corrosion current densities of the Sn3.5Ag0.5Cu solders and Sn3.5Ag0.5Cu nano-composite solders were very similar.

Solder	Φcorr (mV_{SCE})	Φb (mV_{SCE})	$\Delta\Phi$ (mV)	*I*corr ($\mu A/cm^2$)
Sn3.5Ag0.5Cu	-662.1	-284.1	378	0.36
Sn3.5Ag0.5Cu-0.5TiO2	-651.4	-95.1	556	0.27
Sn3.5Ag0.5Cu-0.5Al2O3	-642.1	-146.2	496	0.40

Φcorr : corrosion potential; Icorr: corrosion current density; Φb : breakdown potential;
ΔΦ = Φcorr - Φb.

Table 6. Corrosion properties in a 3.5 wt.% NaCl solution for the nano-composite solder [60].

Many studies have reported that the corrosion behavior of alloys depends on the second phase distribution, shown to be Mg alloy[61, 62] and Al alloy[63]. In the Sn3.5Ag0.Cu nano-composite solder alloys, the microstructure had finer β-Sn grains, a large amount of Ag_3Sn particles, and a small amount of oxidize nanoparticles. This leads to improvement of the corrosion behavior of the Sn3.5Ag0.5Cu nano-composite solder, such as greater corrosion resistance, the lower pitting tendency, and the smaller corrosion current density, respectively.

The corrosion products of Sn3.5Ag0.5Cu and Sn3.5Ag0.5Cu nano-composite solder have similar microstructures (Fig. 15). The corrosion products of Sn3.5Ag0.5Cu solder after polarization have a larger flake-like shape (Mark a) and small mushroom-like shape, and are loosely distributed on the surface, with different orientations (Fig.15a). On the other hand, the corrosion products of Sn3.5Ag0.5Cu nano-composite solder after polarization tests have only a flake-like shape, as shown in Fig. 15b (Mark a). Table 7 shows the surface element concentrations of solder corrosion products from EDS. According to the EDS analysis, the corrosion products of Sn3.5Ag0.5Cu and Sn3.5Ag0.5Cu nano-composite solder contain mainly Sn, O, and Cl (Fig.16). It can be seen that the corrosion products of the Sn3.5Ag0.5Cu solders and Sn3.5Ag0.5Cu nano-composite solders have slightly different compositions.

Solder		Surface element concentration (wt.%)				
		Sn	Ag	Cu	Cl	O
Sn3.5Ag0.5Cu	All area	69.26	4.05	0.37	13.40	12.60
	flake	72.97	0.43	-	15.71	9.58
	mushroom	74.87	1.29	-	17.97	5.76
Sn3.5Ag0.5Cu-0.5TiO_2	All area	68.7	3.82	0.68	13.39	13.41
	flake	64.22	0.50		15.03	20.25

Table 7. Surface element concentration of different solders after potentiodynamic polarization tests[60].

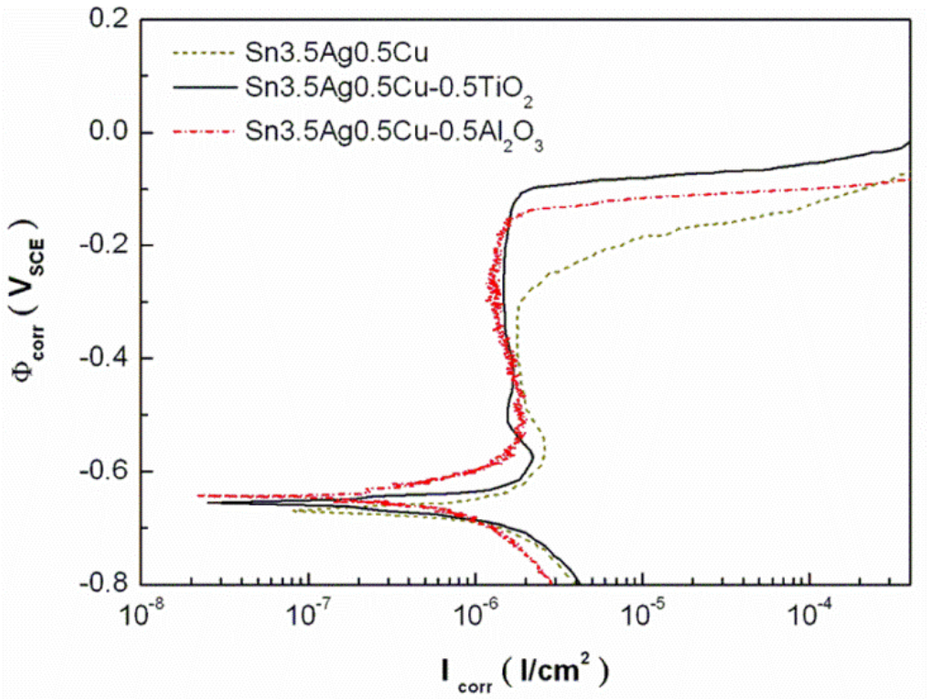


Fig. 14. The potentiodynamic polarization curves of the nano-composite solder in a 3.5wt.% NaCl solution: (a) Sn3.5Ag0.5Cu solder; (b) Sn3.5Ag0.5Cu-0.5TiO_2; and (c) Sn3.5Ag0.5Cu-0.5Al_2O_3 [60].

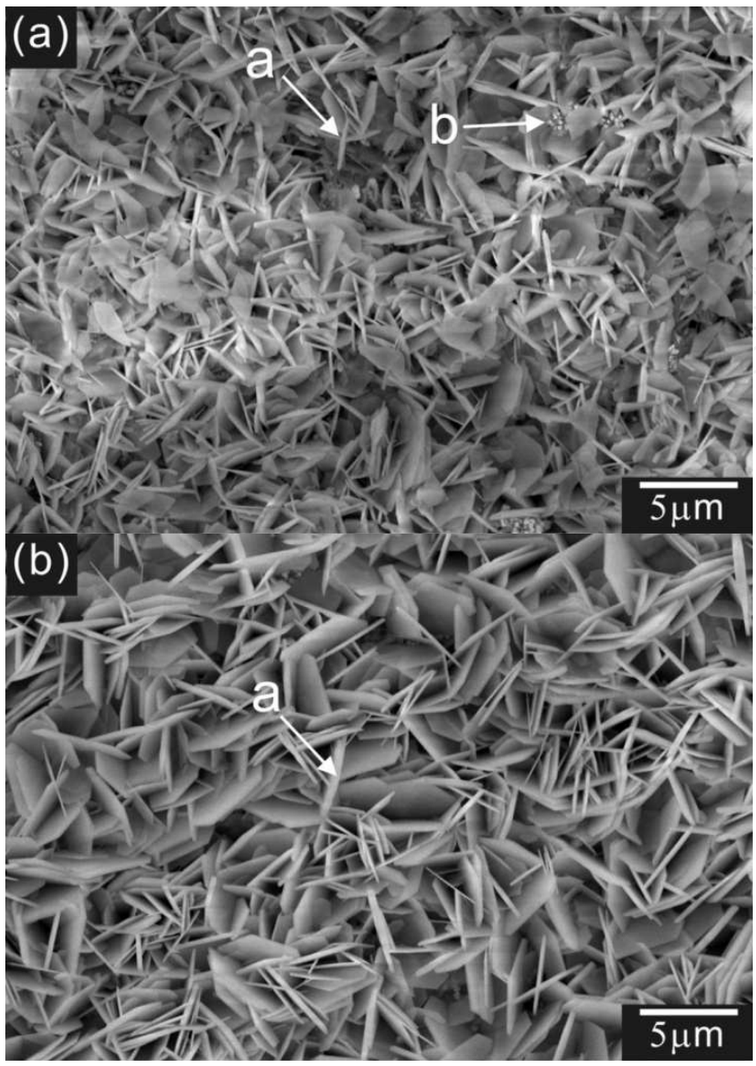


Fig. 15. Microstructure of the corrosion products on different solders after polarization tests (a) Sn3.5Ag0.5Cu solder, (b) Sn3.5Ag0.5Cu nano-composite solder[60].

During polarization testing in NaCl solution, the only possible cathodic reaction is oxygen reduction [49, 64]:

$$O_2 + 4e^- + 2H_2 \rightarrow 4OH^- \quad (1)$$

When the current density reaches about 10 mA/cm², many hydrogen bubbles evolve from the cathode due to the hydrogen evolution on the cathode:

$$2H_2O + 2e^- \rightarrow H_2 + 2OH^- \quad (2)$$

The reactions on the anode are quite complicated. Some possible anodic reactions have been reported in the literature [46, 64-66], as displayed below:

$$Sn + 2OH^- - 2e^- = Sn(OH)_2 \quad (3)$$

$$Sn + 2OH^- - 2e^- = SnO + H_2O \quad (4)$$

$$Sn + 4H_2O = Sn(OH)_4 + 4e^- + 4H^+ \quad (5)$$

The dehydration of $Sn(OH)_2$ and $Sn(OH)_4$ into SnO and SnO_2, respectively, has also been reported [46, 64,65]:

$$Sn(OH)_2 + 2OH^- + 2e^- = Sn(OH)_4 \quad (6)$$

$$Sn(OH)_2 + 2OH^- = SnO + H_2O \quad (7)$$

$$SnO + H_2O + 2OH^- + 2e^- = Sn(OH)_4 \quad (8)$$

However, Yu et al., after investigating the corrosion properties of Sn9Zn and Sn8Zn3Bi solder in NaCl solution, postulated the formation of a tin oxyhydroxychloride according to the following reaction[66]:

$$3Sn + 4OH^- + 2Cl^- = Sn_3O(OH)_2Cl_2 + H_2O \quad (9)$$

In addition, Li et al.[46] studied the corrosion properties of Sn-Ag, Sn–Ag–Cu, Sn–Cu, and SnPb solder in 3.5wt.% NaCl solution with different scanning rates, and their results showed that the corrosion product on the surface was tin oxide chloride hydroxide ($Sn_3O(OH)_2Cl_2$). In our case, the presence of such a surface layer, instead of a tin oxychloride layer, cannot be ruled out due to the detection limits of energy-dispersive spectroscopy. In order to understand the reaction during the corrosion products, XRD has been used to analyse the corrosion products on the surface after the polarization tests (Fig. 17). The results show that all the Sn3.5Ag0.5Cu and Sn3.5Ag0.5Cu solder materials have the same corrosion product, $Sn_3O(OH)_2Cl_2$, which is a complex oxide chloride hydroxide of tin[67]. This further confirms that the corrosion product on the Sn3.5Ag0.5Cu composite solders is $Sn_3O(OH)_2Cl_2$.

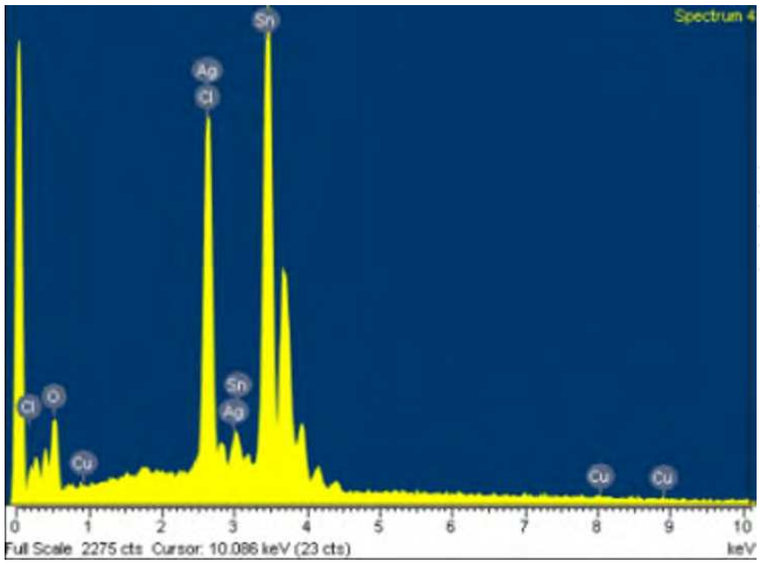


Fig. 16. EDS analysis of corrosion product of the Sn3.5Ag0.5Cu nano-composite solder after polarization tests[60].

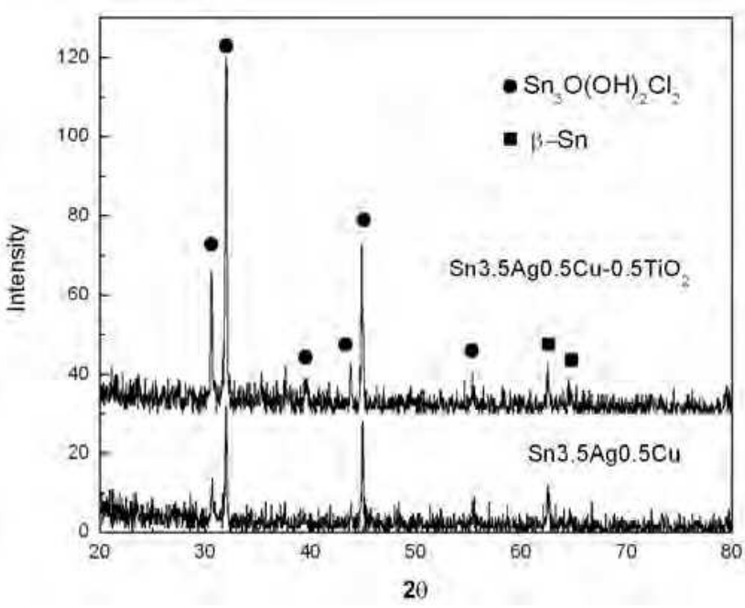


Fig. 17. XRD spectra of different solder materials after polarization tests[60].

9. References

[1] K. N. Tu, K. Zeng, Tin–lead (Sn–Pb) solder reaction in flip chip technology, Mater. Sci. Eng. R 34 (1) (2001) 1–58.

[2] E. P. Wood, K.L. Nimmo, In search of new lead-free electronic solders, J. Electron. Mater. 23 (8) (1994) 709–713.

[3] S. Jin, D. R. Frear, J.W. Morris Jr. Foreword, J. Electron. Mater. 23 (8) (1994) 709-713.

[4] M. Abtew, G. Selvaduray, Lead-free Solders in Microelectronics, Mater. Sci. Eng. R 27 (2000) 95-141.

[5] I. E. Anderson, J. C. Foley, B. A. Cook, J. Harringa, R. L. Terpstra, O. Unal, Alloying effects in near-eutectic Sn–Ag–Cu solder alloys for improved microstructural stability, J. Electron. Mater. 30 (9) (2001) 1050–1059.

[6] M. McCormack, S. Jin, G.W. Kammlott, H. S. Chen, New Pb-free solder alloy with superior mechanical properties, Appl. Phys. Lett. 63 (1) (1993) 15–17.

[7] A. Z. Miric, A. Grusd, Lead-free alloys, Soldering, Surf. Mount Technol. 10 (1) (1998) 19–25.

[8] N. C. Lee, Lead-free Soldering. In Daniel, L. and Wong, C. P. (eds.), Materials for Advanced Packaging, Springer Science Business Media (New York, 2009), pp. 181-218.

[9] K. N. Tu, A.M. Gusak, M. Li, Physics and materials challenges for lead-free solders, J. Appl. Phys. 93 (2003)1335–1353.

[10] H. T. Ma, J. C. Suhling, A review of mechanical properties of lead-free solder for electronic packaging, J. Mater. Sci. 44(2009) 1141–1158.

[11] International Technology Roadmap for Semiconductors—Assembly and Packaging, 2009 ed.
(http://www.itrs.net/Links/2009ITRS/2009Chapters_2009Tables/2009_Assembly.pdf).

[12] E. C. C. Yeth, W. J. Choi, K. N. Tu, Current Crowding Induced Electromigration Failure in Flip Chip Technology, Appl. Phys. Lett. 80 (2002) 580-582.
[13] J. Shen, Y. C. Chan, Research advances in nano-composite solders, Microelectronics Reliability 49 (2009) 223–234.
[14] L. C. Tsao, S. Y. Chang, Effects of Nano-TiO_2 additions on thermal analysis, microstructure and tensile properties of Sn3.5Ag0.25Cu solder, Mater. Des. 31(2010) 990–993.
[15] L. C. Tsao, S.Y. Chang, C.I. Lee, W.H. Sun, C.H. Huang, Effects of nano-Al_2O_3 additions on microstructure development and hardness of Sn3.5Ag0.5Cu solder, Mater. Des. 31, (2010) 4831–4835.
[16] T. H. Chuang, M. W. Wu, S. Y. Chang, S. F. Ping, L. C. Tsao, Strengthening mechanism of nano-Al_2O_3 particles reinforced Sn3.5Ag0.5Cu lead-free solder, J. Mater. Sci.: Mater. Electron. 22 (2011)1021–1027.
[17] J. Shen, Y.C. Liu, D. J. Wang, H.X. Gao, Nano ZrO_2 particulate-reinforced lead-free solder composite, J. Mater. Sci. Technol. 22 (2006) 529-532.
[18] X. L. Zhong, M. Gupta, Development of lead-free Sn–0.7Cu/Al_2O_3 nanocomposite solders with superior strength, J. Phys. D: Appl. Phys. 41 (2008) 095403–095409.
[19] K. Mohan Kumar, V. Kripesh, Andrew A.O. Tay, Single-wall carbon nanotube (SWCNT) functionalized Sn–Ag–Cu lead-free composite solders, J. Alloy Compd. 450 (2008) 229–237.
[20] S. M. L. Nai, J. Wei, M. Gupta, Improving the performance of lead-free solder reinforced with multi-walled carbon nanotubes, Mater. Sci. Eng. A 423 (2006) 166–169.
[21] S. M. L. Nai, J. Wei, M. Gupta, Influence of ceramic reinforcements on the wettability and mechanical properties of novel lead-free solder composites, Thin Solid Films 504 (2006) 401–404.
[22] Z. X. Li, M. Gupta, High strength lead-free composite solder materials using nano-Al_2O_3 as reinforcement. Adv. Eng. Mater. 7 (2005)1049–1054.
[23] S. M. L. Nai, J. Wei, M. Gupta, Effect of carbon nanotubes on the shear strength and electrical resistivity of a lead-free solder. J. Electron. Mater. 37(2008) 515–522.
[24] H. Mughrabi, Plastic deformation and fracture of materials. Berlin: Springer-Verlag;. 1993. p. 315–322
[25] L. C. Tsao, 10th International Conference on Electronic Packaging. Technology & High Density Packaging (ICEPT-HDP 2009) (2009)1164 -1166.
[26] R. W. Wu, L. C. Tsao, S. Y. Chang, C. C. Jain and R. S. Chen, Interfacial reactions between liquid Sn3.5Ag0.5Cu solders and Ag substrates, J. Mater. Sci.: Mater. Electron. 22(8) (2011) 1181-1187.
[27] Görlich, D. Baither, G. Schmitz, Reaction kinetics of Ni/Sn soldering reaction, Acta Materialia 58(9) (2010) 3187-3197.
[28] T. H. Chuang, Y. T. Huang, L. C. Tsao, $AgIn_2$/Ag_2In transformations in an In-49Sn/Ag soldered joint under thermal aging, J. Electron. Mate. 30 (2001) 945-950.
[29] D. G. Kim, C. Y. Lee, S. B. Jung, Interfacial reactions and intermetallic compound growth between indium and copper, J. Mater. Sci.: Mater. Electron. 5(2) (2004) 95-98.
[30] L. C. Tsao, Evolution of nano-Ag_3Sn particle formation on Cu–Sn intermetallic compounds of Sn3.5Ag0.5Cu composite solder/Cu during soldering, J. Alloy Compd.509 (2011) 2326–2333.

[31] L. C. Tsao, Suppressing effect of 0.5 wt.% nano-TiO_2 addition into Sn–3.5Ag–0.5Cu solder alloy on the intermetallic growth with Cu substrate during isothermal aging, J. Alloy Compd. 509 (2011) 8441– 8448.
[32] L. C. Tsao, C.P. Chu, S. F. Peng, Study of interfacial reactions between Sn3.5Ag0.5Cu composite alloys and Cu substrate, Microelectron. Eng. 88 (2011) 2964-2969.
[33] S. Y. Chang, L. C. Tsao, M. W. Wu and C. W. Chen, The morphology and kinetic evolution of intermetallic compounds at Sn–Ag–Cu solder/Cu and Sn–Ag–Cu-0.5Al_2O_3 composite solder/Cu interface during soldering reaction, J. Mater. Sci.: Mater. Electron. DOI: 10.1007/s10854-011-0476-9.
[34] X.Y. Liu, M.L. Huang, C. M. L. Wu, Lai Wang, Effect of Y_2O_3 particles on microstructure formation and shear properties of Sn-58Bi solder, J Mater Sci: Mater Electron, J Mater Sci: Mater Electron 21 (2010) 1046–1054.
[35] S. M. L. Nai, J. Wei, M. Gupta, Interfacial Intermetallic Growth and Shear Strength of Lead-Free Composite Solder Joints, J. Alloy Compd. 473 (2009) 100–106.
[36] A. K. Gain, T. Fouzder, Y. C. Chan, Winco K. C. Yung, Microstructure, kinetic analysis and hardness of Sn–Ag–Cu–1 wt% nano-ZrO_2 composite solder on OSP-Cu pads, J. Alloy Compd. 509 (2011) 3319–3325.
[37] R. Ambat, P. Møller, A review of Corrosion and environmental effects on electronics, The Technical University of Denmark, DMS vintermøde proceedings, (2006).
[38] M. Mori, K. Miura, Corrosion of Tin Alloys in ulfuric and Nitric Acids, Corrosion Science, 44 (2002)887-898.
[39] F. Song, S. W. Ricky Lee, Corrosion of Sn-Ag-Cu Lead-free Solders and the Corresponding Effects on Board Level Solder Joint Reliability, 2006 Electronic Components and Technology Conference, (2006) 891-889.
[40] B. Liu, T. K. Lee, K. C. Liu, Impact of 5% NaCl Salt Spray Pretreatment on the Long-Term Reliability of Wafer-Level Packages with Sn-Pb and Sn-Ag-Cu Solder Interconnects , J. Electron. Mater. 40, 2011,doi: 10.1007/s11664-011-1705-y.
[41] Morten S. Jellesen et al., Corrosion in Electronics (Paper presented at 2008 Eurocorr Conference, Edinburgh, Scotland, 7–11 September 2008).
[42] R. Baboian, "Electronics," Corrosion Tests and Standards: Applications and Interpretation, ed. R. Baboian (West Conshohocken, PA: ASTM, 1996), www .corrosionsource. com/events/intercorr/baboian.htm).
[43] V. Chidambaram, J. Hald, R. Ambat, J. Hattel,A Corrosion Investigation of Solder Candidates for High-temperature Applications, JOM , 61 (2009) 59-65.
[44] H. Liu, K. Wang, K. Aasmundtveit, N. Hoivik, Intermetallic Cu_3Sn as Oxidation Barrier for Fluxless Cu-Sn Bonding, 2010 Electronic Components and Technology Conference, 853-857.
[45] L. C. Tsao, Corrosion Characterization of Sn37Pb Solders and With Cu Substrate Soldering Reaction in 3.5wt.% NaCl Solution, 2009 International Conference on Electronic Packaging Technology & High Density Packaging (ICEPT-HDP), (2009) 1164-1166.
[46] D. Li, P. P. C. C. Liu, Corrosion characterization of tin–lead and lead free solders in 3.5 wt.% NaCl solution, Corr. Sci. 50 (2008) 995–1004.
[47] K. L. Lin, T.P. Liu, The electrochemical corrosion behaviour of. Pb-Free Al–Zn–Sn solders in NaCl solution, Mater. Chem. Phys. 56 (1998) 171-176.

[48] K. L. Lin, F.C. Chung, T.P. Liu, The potentiodynamic polarization behavior of Pb-free XIn-9(5Al-Zn)-YSn solders, Mater. Chem. Phys. 53 (1998) 55-59.
[49] U.S. Mohanty, K.L. Lin, The effect of alloying element gallium on the polarisation characteristics of Pb-free Sn–Zn–Ag–Al–XGa solders in NaCl solution, Corros. Sci. 48 (2006) 662–678.
[50] D. Q. Yu, W. Jillek, E. Schmitt, Electrochemical migration of Sn–Pb and lead free solder alloys under distilled water, J. Mater. Sci. :Mater. Electron. 17 (2006) 219–227.
[51] B. Y. Wu, Y.C. Chan, M. O. Alam, Electrochemical corrosion study of Pb-free solders, J. Mater. Res. 21 (2006) 62-70.
[52] A. Ahmido, A. Sabbar, H. Zouihri, K. Dakhsi, F. Guedira, M. Serghini-Idrissi, S. El Hajjaji ,Effect of bismuth and silver on the corrosion behavior of Sn–9Zn alloy in NaCl 3wt.% solution, Mater. Sci. Eng. B 176 (2011) 1032– 1036.
[53] U. S. Mohanty, K. L. Lin, Electrochemical corrosion behaviour of Pb-free Sn-8.5Zn-0.05Al-XGa and Sn-3Ag-0.5Cu alloys in chloride containing aqueous solution, Corrosion Science 50 (2008) 2437–2443.
[54] J. Hu, T. Luo, A. Hu, M. Li, D. Mao, Electrochemical Corrosion Behaviors of Sn-9Zn-3Bi-xCr Solder in 3.5% NaCl Solution, J. Electron. Mater. 40, (2011) 1556-1562.
[55] T. C. Chang, J. W. Wang, M. C. Wang , M. H. Hon, Solderability of Sn-9Zn-0.5Ag-1In lead-free solder on Cu substrate Part 1. Thermal properties, microstructure, corrosion and oxidation resistance, J. Alloy Compd. 422 (2006) 239–243.
[56] F. Rosalbino, E. Angelini, G. Zanicchi, R. Marazza, Corrosion behaviour assessment of lead-free Sn-Ag-M (M = In, Bi, Cu) solder alloys, Mater. Chem. Phys. 109 (2008) 386–391.
[57] T. H. Chuang, M. W. Wu , S. Y. Chang, S. F. Ping, L. C. Tsao, Strengthening mechanism of nano-Al_2O_3 particles reinforced Sn3.5Ag0.5Cu lead-free solder, J Mater Sci: Mater Electron 22 (2011) 1021–1027.
[58] J. C. Leong , L. C. Tsao , C. J. Fang,C. P. Chu, Effect of nano-TiO_2 addition on the microstructure and bonding strengths of Sn3.5Ag0.5Cu composite solder BGA packages with immersion Sn surface finish, J Mater Sci: Mater Electron, (2011)1443-1449.
[59] L. C. Tsao, M. W. Wu, S. Y. Chang, Effect of TiO_2 nanoparticles on the microstructure and bonding strengths of Sn0.7Cu composite solder BGA packages with immersion Sn surface finish, J Mater Sci: Mater Electron DOI 10.1007/s10854-011-0471-1.
[60] L. C. Tsao, T. T. Lo, S. F. Peng, S. Y. Chang, Electrochemical behavior of a new Sn3.5Ag0.5Cu composite solder, 11th International Conference on Electronic Packaging Technology & High Density Packaging, (2010), 1013-1017.
[61] A. Pardo, M. C. Merino, A. E. Coy, R. Arrabal, F. Viejo, E. Matykina, Corrosion Behavior of Magnesium/Aluminum Alloys in 3.5 wt% NaCl, Corr. Sci., 50 (2008)823-834.
[62] G. Ben-Hamu, A. Eliezer, E. M.Gutman. Electrochemical Behavior of Magnesium Alloys strained in Buffer Solutions, Electrochim. Acta, 52 (2006)304-313.
[63] Y. Liu, Y. F. Cheng, Role of Second Phase Particles in Pitting Corrosion of 3003 Al Alloy in NaCl Solution, Mater. Corr., 61 (2010)211-217.
[64] S. D. Kapusta, N. Hackerman, Anodic passivation of tin in slightly alkaline solutions, Electrochim. Acta 25 (1980) 1625–1639.
[65] Q. V. Bui, N. D. Nam, B.I. Noh, A. Kar, J. G. Kim, S.B. Jung, Effect of Ag addition on the corrosion properties of Sn-based solder alloys, Mater. Corr. 61 (2010) 30-33.

[66] D. Q. Yu, C. M. L. Wu, L. Wang, The Electrochemical Corrosion Behavior of Sn-9Zn and Sn-8Zn-3Bi Lead-Free Solder Alloys in. NaCl Solution, 16th International Corrosion Congress, Beijing, P.R. China, (2005)19–24.
[67] F. Rosalbino, E. Angelini, G. Zanicchi, R. Carlini, R. Marazza, Electrochemical Corrosion Study of Sn–3Ag–3Cu Solder Alloy in NaCl solution, Electrochim. Acta, 54 (2009) 7231-7237.

IntechOpen

IntechOpen



Corrosion Resistance

Edited by Dr Shih

ISBN 978-953-51-0467-4
Hard cover, 472 pages
Publisher InTech
Published online 30, March, 2012
Published in print edition March, 2012

The book has covered the state-of-the-art technologies, development, and research progress of corrosion studies in a wide range of research and application fields. The authors have contributed their chapters on corrosion characterization and corrosion resistance. The applications of corrosion resistance materials will also bring great values to reader's work at different fields. In addition to traditional corrosion study, the book also contains chapters dealing with energy, fuel cell, daily life materials, corrosion study in green materials, and in semiconductor industry.

How to reference

In order to correctly reference this scholarly work, feel free to copy and paste the following:

L.C. Tsao (2012). Corrosion Resistance of Pb-Free and Novel Nano-Composite Solders in Electronic Packaging, Corrosion Resistance, Dr Shih (Ed.), ISBN: 978-953-51-0467-4, InTech, Available from: http://www.intechopen.com/books/corrosion-resistance/corrosion-resistance-of-pb-free-and-novel-nano-composite-solders-in-electronic-packaging

INTECH
open science | open minds

InTech Europe
University Campus STeP Ri
Slavka Krautzeka 83/A
51000 Rijeka, Croatia
Phone: +385 (51) 770 447
Fax: +385 (51) 686 166
www.intechopen.com

InTech China
Unit 405, Office Block, Hotel Equatorial Shanghai
No.65, Yan An Road (West), Shanghai, 200040, China
中国上海市延安西路65号上海国际贵都大饭店办公楼405单元
Phone: +86-21-62489820
Fax: +86-21-62489821

© 2012 The Author(s). Licensee IntechOpen. This is an open access article distributed under the terms of the Creative Commons Attribution 3.0 License, which permits unrestricted use, distribution, and reproduction in any medium, provided the original work is properly cited.

IntechOpen

IntechOpen